ELSEVIER

Available online at www.sciencedirect.com

SCIENCE DIRECT®

Applied Surface Science 224 (2004) 87–90

applied surface science

www.elsevier.com/locate/apsusc

Segregation of boron to polycrystalline and single-crystal $Si_{1-x-y}Ge_xC_y$ and $Si_{1-y}C_y$ layers

E.J. Stewart*, J.C. Sturm

Center for Photonics and Optoelectronic Materials, Department of Electrical Engineering, Princeton University, Princeton, NJ 08544, USA

Abstract

Strong boron segregation to polycrystalline $Si_{1-x-y}Ge_xC_y$ alloys from Si has previously been reported [MRS Symp. Proc. 669 (2001) J6.9]. In this study, we investigate potential mechanisms for this effect. We find that comparable segregation also occurs in both polycrystalline $Si_{1-y}C_y$ and single-crystal $Si_{1-x-y}Ge_xC_y$, indicating neither Ge nor grain boundary effects are needed for it to occur. In addition, the stability of the electrical properties of polycrystalline $Si_{1-x-y}Ge_xC_y$ with annealing suggests that inactive B–C defects are not forming. Point defect gradients are presented as a mechanism consistent with the electrical data.
© 2003 Elsevier B.V. All rights reserved.

PACS: 68.55.Ln

Keywords: Boron; Segregation; Diffusion; $Si_{1-x-y}Ge_xC_y$; Polycrystalline

1. Introduction

Understanding dopant transport in $Si_{1-x-y}Ge_xC_y$ and $Si_{1-y}C_y$ alloys is important for the integration of these materials in modern devices such as MOSFETs and HBTs. Previously, it has been shown that boron strongly segregates to polycrystalline $Si_{1-x-y}Ge_xC_y$ layers from Si [1]. This effect is more pronounced than previous reports of boron segregation to single crystal $Si_{1-x}Ge_x$ [2,3], and increases with increasing carbon content. It has been exploited to make polycrystalline $Si_{1-x-y}Ge_xC_y$-gated MOSFETs with increased resistance to boron penetration compared to either poly Si or $Si_{1-x}Ge_x$ gated devices [4]. This work examines the mechanism driving this segregation. We show that a similar segregation effect occurs in both polycrystalline $Si_{1-y}C_y$ (no Ge) and single crystal $Si_{1-x-y}Ge_xC_y$, indicating that neither Ge, nor any polycrystalline effects (i.e. grain boundary defects), are needed for it to occur. In addition, the electrical properties of polycrystalline $Si_{1-x-y}Ge_xC_y$ indicate that inactive B–C related defects are not forming. We discuss point-defect gradients as a possible mechanism driving this segregation.

2. Segregation in $Si_{1-x-y}Ge_xC_y$ and $Si_{1-y}C_y$

All structures used in this study were grown by Rapid Thermal Chemical Vapor Deposition at temperatures between 625 °C and 750 °C, using $SiCl_2H_2$, SiH_4, and Si_2H_6 as silicon sources and GeH_4, $SiCH_6$, and B_2H_6 as germanium, carbon, and boron sources, respectively. Two polycrystalline $Si_{1-y}C_y$ (no Ge)

* Corresponding author. Tel.: +1-609-258-6624; fax: +1-609-258-1840.
E-mail address: estewart@princeton.edu (E.J. Stewart).

0169-4332/$ – see front matter © 2003 Elsevier B.V. All rights reserved.
doi:10.1016/j.apsusc.2003.08.044

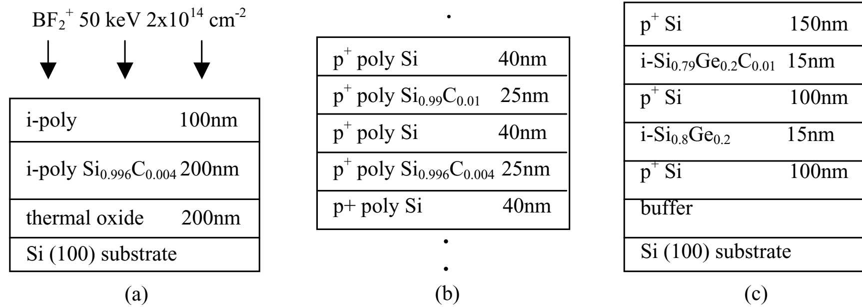

Fig. 1. Structures of: (a) two-layer polycrystalline $Si/Si_{1-y}C_y$ sample, (b) multi-layer poly $Si/Si_{1-y}C_y$ sandwich structure, and (c) single-crystal multi-layer sandwich structure.

structures were fabricated, shown in Fig. 1 (a) and (b), to study the importance of Ge in the segregation process. Growth parameters for the $Si_{1-y}C_y$ layers were chosen to incorporate carbon on substitutional lattice sites [5]. The first structure consisted of 200 nm of undoped poly $Si_{1-y}C_y$ underneath 100 nm of undoped poly Si, all on a thermally oxidized Si substrate. Boron was implanted into the top poly Si layer by BF_2^+ at $2 \times 10^{14}\ cm^{-2}$ and 50 keV. To drive the dopant into the underlying poly $Si_{1-y}C_y$, a 900 °C, 4 h anneal was performed. Fig. 2 shows SIMS profiles of this sample after the anneal. Boron has segregated into the poly $Si_{1-y}C_y$ layer, with a segregation coefficient $m = [B]_{poly\,SiC}/[B]_{poly\,Si} = 1.5$ (longer anneals performed on similar poly $Si/Si_{1-x-y}Ge_xC_y$ structures do not show any more increase in the segregation). This value is comparable to that of poly $Si_{1-x-y}Ge_xC_y$ layers with similar C content, indicating that Ge is not required for segregation.

The second sample was a multi layer structure that included two poly $Si_{1-y}C_y$ (0.4% and 1%) layers sandwiched between poly Si layers. This sample was in situ doped with boron during growth at a much higher level than the previous sample, $\sim 7 \times 10^{20}\ cm^{-3}$. An 800 °C, 22 h anneal was performed to allow for dopant redistribution, and SIMS profiles taken before and after the anneal (Fig. 3). For the 0.4% layer, segregation is similar to the previous sample, $m = 1.3$. A larger effect is seen in the 1% layer, with $m = 1.8$. Again, segregation is observed without Ge even at very high doping levels, and increases with increasing carbon content.

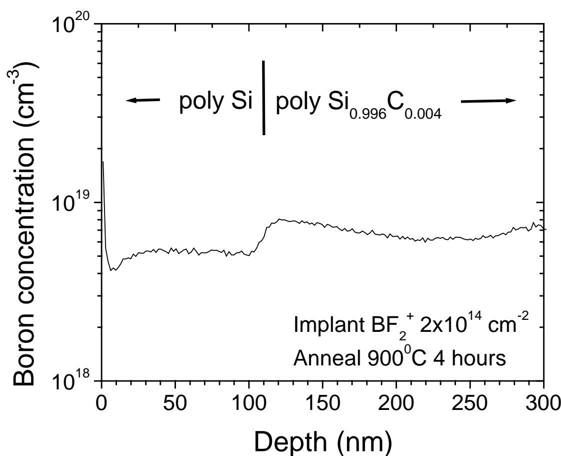

Fig. 2. SIMS profile of implanted two-layer poly $Si/Si_{0.996}C_{0.004}$ sample, showing boron segregation to poly $Si_{0.996}C_{0.004}$ layer after a 900 °C, 4 h anneal.

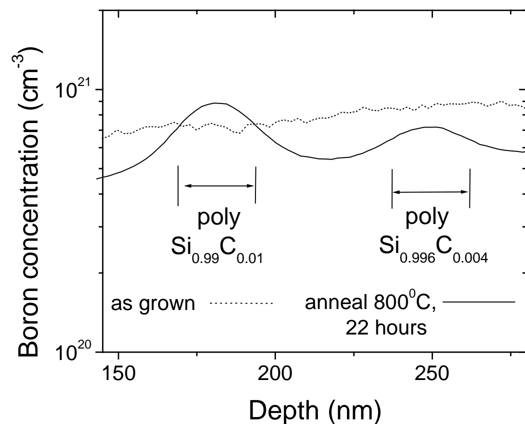

Fig. 3. SIMS profile of multi-layer in situ doped poly $Si/Si_{1-y}C_y$ sandwich structure, showing increasing segregation at higher carbon levels.

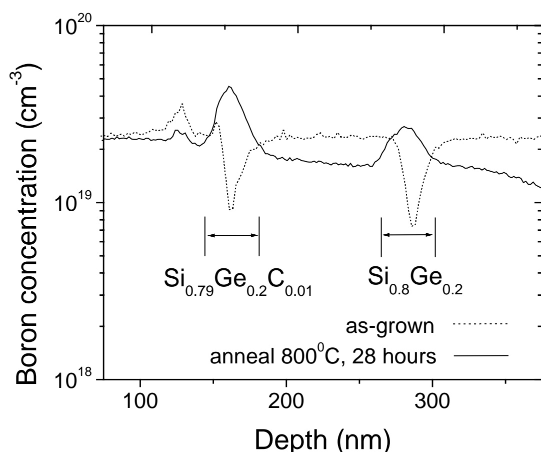

Fig. 4. SIMS profile of single-crystal Si/$Si_{1-x-y}Ge_xC_y$ sandwich structure, showing increased boron segregation into $Si_{0.79}Ge_{0.2}C_{0.01}$ vs. $Si_{0.8}Ge_{0.2}$.

A third sample was grown to investigate segregation in single crystal material, shown in Fig. 1(c). On top of an n-type substrate and buffer, thin (~15 nm) epitaxial layers of undoped $Si_{1-x}Ge_x$ and $Si_{1-x-y}Ge_xC_y$ were sandwiched between thicker (~100 nm) doped Si layers ($[B] = 2 \times 10^{19}\,cm^{-3}$). This structure was capped with deposited SiO_2 and annealed at 800 °C for 28 h to allow boron to move into the $Si_{1-x}Ge_x$ and $Si_{1-x-y}Ge_xC_y$ layers. Fig. 4 shows SIMS of this structure before and after annealing. The as-grown profile shows a boron peak outside the $Si_{1-x-y}Ge_xC_y$ layers at ~20 nm, which was unintentionally incorporated during growth and should not have an effect on the rest of the experiment. Boron segregation into the $Si_{1-x}Ge_x$ layer ($m = 1.7$) is observed as anticipated, and comparable to reported values [2,3]. However, additional segregation occurs in the $Si_{1-x-y}Ge_xC_y$ layer ($m = 2.3$), revealing that carbon also enhances boron segregation in single-crystal material. Polycrystalline effects (i.e. grain boundary defects) are not (at least completely) responsible for the previously observed segregation to poly $Si_{1-x-y}Ge_xC_y$.

3. Discussion

Several mechanisms have been proposed to explain boron segregation in single-crystal strained $Si_{1-x}Ge_x$ (no C) versus Si. These include relieving strain energy, electronic energy differences due to the smaller band gap of $Si_{1-x}Ge_x$ versus Si [6], and direct Ge–B interactions [7]. When small amounts of substitutional carbon are added to $Si_{1-x}Ge_x$ commensurate on Si, the carbon is known to lead to less macroscopic strain and a larger band gap than $Si_{1-x}Ge_x$, both of which would predict less segregation of boron to $Si_{1-x-y}Ge_xC_y$ layers. This is the opposite of what is observed. In addition, the observation of segregation to $Si_{1-y}C_y$ layers indicates that carbon itself can drive the segregation, without any Ge–B effects.

Another possibility is that direct B–C interactions are responsible. For example, Liu et al. proposed an immobile boron-carbon-interstitial cluster [8]. In this case, one might expect to see a degradation of the electrical properties upon annealing (assuming the B–C defects render the boron inactive). Fig. 5 shows the resistivity of polycrystalline $Si_{1-x-y}Ge_xC_y$ layers (compared to poly Si and $Si_{1-x}Ge_x$) annealed at 900 °C for a long time (all layers were in situ doped at $\sim 1 \times 10^{19}\,cm^{-3}$). While the as-grown poly $Si_{1-x-y}Ge_xC_y$ does have a higher resistivity versus the poly $Si_{1-x}Ge_x$, no increase is observed during the anneal, even out to 24 h (much longer than the time scale required to allow for segregation). This suggests that inactive defects are not responsible for the segregation.

Point defect gradients represent another possible driving mechanism. Boron diffusion in Si has been shown to be mediated by Si interstitials. The equation for boron diffusion flux can be expressed as [9]:

$$F_B = -D_B \frac{d([B](I/I_0))}{dx}$$

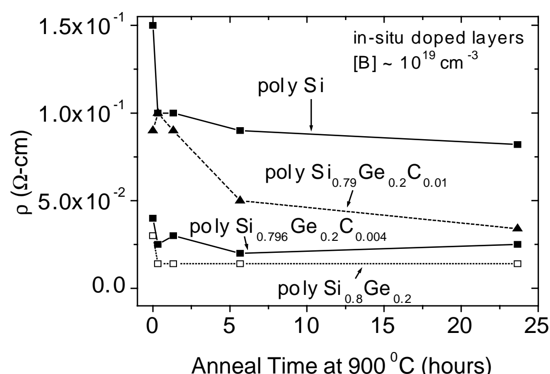

Fig. 5. Resistivity of in situ doped poly Si, poly $Si_{1-x}Ge_x$, and poly $Si_{1-x-y}Ge_xC_y$ layers vs. anneal time.

where F_B is the diffusion flux of boron atoms, [B] is the concentration of boron, D_B is the equilibrium diffusivity of boron, and I/I_0 is the ratio of Si interstitials to the equilibrium value. If the interstitial profile varies with position, the equation becomes:

$$F_B = -D_B\left(\frac{I}{I_0}\right)\frac{d[B]}{dx} - D_B[B]\frac{d(I/I_0)}{dx}$$

The first term is the usual diffusion flux due to a concentration gradient, while the second term represents a flux of boron atoms due to an interstitial gradient, even if no gradient exists in the boron profile. $Si_{1-x-y}Ge_xC_y$ and $Si_{1-y}C_y$ layers are known to locally suppress the concentration of interstitials [10]. If the interstitial concentration is decreased in a region, then an additional driving force exists for boron to move to that region, producing a segregation effect. As this mechanism does not require the presence of inactive B–C defects, it is consistent with the results of the electrical measurements. Further experiments are underway to confirm this conclusion.

4. Summary

In conclusion, we have investigated different mechanisms to explain boron segregation in polycrystalline $Si_{1-x-y}Ge_xC_y$ alloys. Comparable effects are seen in both polycrystalline $Si_{1-y}C_y$ and single crystal $Si_{1-x-y}Ge_xC_y$, indicating neither Ge nor grain boundary effects are necessary. Stability of the electrical properties of polycrystalline $Si_{1-x-y}Ge_xC_y$ with annealing suggests that inactive B–C related defects are not forming. Point defect gradients are presented as a mechanism consistent with the electrical data.

Acknowledgements

This work was supported by DARPA/ONR N660001-97-8904 and ARO DAA655-98-1-0270.

References

[1] E.J. Stewart, M.S. Carroll, J.C. Sturm, MRS Symp. Proc. 669 (2001) J6.9.
[2] S.M. Hu, D.C. Ahlgren, P.A. Ronsheim, J.O. Chu, Phys. Rev. Lett. 67 (1991) 1450–1453.
[3] T.T. Fang, W.T.C. Fang, P.B. Griffin, J.D. Plummer, Appl. Phys. Lett. 68 (6) (1996) 791–793.
[4] E.J. Stewart, M.S. Carroll, J.C. Sturm, IEEE Electron Device Lett. 22 (12) (2001) 574–576.
[5] M.S. Carroll, J.C. Sturm, Appl. Phys. Lett. 81 (7) (2002) 1225–1227.
[6] S.M. Hu, Phys. Rev. B 45 (8) (1992) 4498–4501.
[7] R.F. Lever, J.M. Bonar, A.F.W. Willoughby, J. Appl. Phys. 83 (4) (1998) 1988–1994.
[8] C.-L. Liu, W. Windl, L. Borucki, S. Lu, X.Y. Liu, Appl. Phys. Lett. 80 (1) (2002) 52–54.
[9] C.S. Rafferty, H.-H. Vuong, S.A. Eshraghi, M.D. Giles, M.R. Pinto, S.J. Hillenius, IEDM Tech. Digest (1993) 311–314.
[10] R. Scholz, U. Gosele, J-Y. Huhm, T.Y. Tan, Appl. Phys. Lett. 72 (2) (1998) 200–202.